ISBN: 978-3-95450-247-9 ISSN: 2673-5490 doi: 10.18429/JACoW-IPAC2024-TUAN3

UNDERSTANDING OF THE LHC WARM VACUUM MODULE HEATING

P. Krkotić*, C. Antuono[1†], V. Baglin, G. Bregliozzi, S. Calatroni, P. Chiggiato, E. de la Fuente[2], A. Galloro[3], L. Giacomel, Y. Papaphilippou, G. Rumolo, B. Salvant, O. Santos, L. Sito[4], C. Zannini
CERN, Meyrin, Switzerland
[1]also at Sapienza Università di Roma, Rome, Italy
[2]also at Universidad Politécnica de Madrid, Madrid, Spain
[3]also at Università della Calabria, Arcavacata, Italy
[4]also at Università degli Studi di Napoli Federico II, Naples, Italy

Abstract

During the third run of the Large Hadron Collider in 2023, which had the highest intensity bunch population compared to previous runs, increased losses attributed to pressure spikes within a warm vacuum sector triggered a beam dump. Subsequent inspections revealed localised annealing and plasticisation of the tension spring in the sliding contact radio-frequency finger module, alongside traces of vapour deposition on the various module components with the stainless-steel spring material. A comprehensive analysis involving vacuum and beam impedance studies was conducted to investigate the triggering mechanisms behind the radio-frequency finger module failure. The findings indicate localised beam-induced heating, which could lead to the annealing of the spring with a consequent cascade of effects. Additionally, investigations of potential mitigation measures were performed.

INTRODUCTION

In the past decade, several components of the Large Hadron Collider (LHC) have encountered challenges stemming from beam-induced heating, particularly when the beam/bunch intensity was increased and/or bunch lengths were reduced [1–4]. As a result, multiple issues led to beam dumps, operational delays, and significant equipment damage. Specifically, in the third operational run of the LHC, when the bunch intensity exceeded for the first time $1.6 \cdot 10^{11}$ p/bunch with 25 ns bunch spacing, a beam dump was triggered by strong losses attributed to pressure spikes, within a warm vacuum sector. Upon subsequent inspections, it was discovered that the root cause of the issue lay within a malfunctioning sliding contact RF finger module with an inner diameter (ID) of 212.7 mm, the so-called ID212 warm modules (WM). The X-ray image in Fig. 1 shows that the tension spring designated to maintain the electrical contact between RF fingers and the central transition tube appears deformed and displaced compared to its nominal position. The exchange of the damaged module caused an LHC downtime of about a week.

The visual inspection after the removal of the module unveiled localised annealing and plasticisation of the tension spring, suggesting temperatures up to 500 °C were reached.

* patrick.krkotic@cern.ch
† chiara.antuono@cern.ch

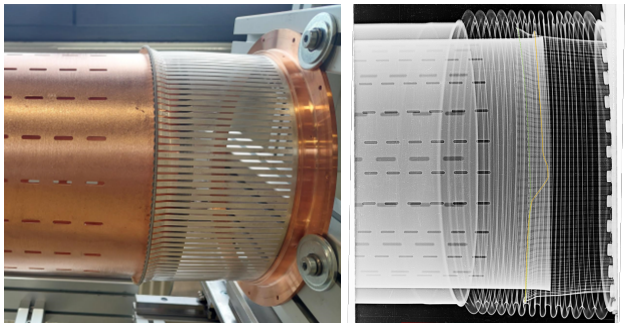

Figure 1: Photograph and X-ray image of the conform and damaged ID212 WM.

Besides, the occurrence of sputtering and sublimation of steel from the tension spring onto other module components were found, indicating the occurrence of sparking.

Following the observation above, an X-ray investigation was conducted on all 71 installed ID212 WMs prior to the 2024 run to identify and mitigate potential risks. Eight ID212 WMs were identified in different sectors around the LHC with degradation in either the tension springs and/or the RF fingers, suggesting an installation position-dependent beam-induced heating effect. This paper outlines the observations and research conducted to understand the ID212 WM breakdown in the LHC and its triggering mechanism.

NON-CONFORMITIES AND HEAT RESISTANCE

The tension spring is composed of stainless steel 1.4310 (AISI 301), known for its robust mechanical properties and potential use in high-temperature environments. As the warm sectors undergo regular bake-out cycles at 250 °C, a tensile test was conducted at different temperatures to probe the tension spring's mechanical behaviour after thermal duress [5]. The study's findings suggested no alterations in spring rates or the tension spring's free lengths at the aforementioned regular bake-out temperatures. Further tests performed at 330 °C showed a subtle but notable stress redistribution. These tests also revealed a modified force-extension relationship, i.e., larger elongations are required to maintain prior contact forces as before the heat treatment.

A case study approach was used to determine the power deposition required to heat the tension spring to temperatures up to annealing conditions of 500 °C [6]. Two distinct simu-

ISBN: 978-3-95450-247-9 ISSN: 2673-5490 doi: 10.18429/JACoW-IPAC2024-TUAN3

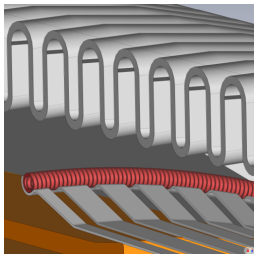

(a) uniform heating

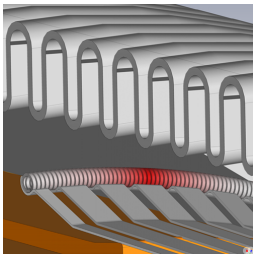

(b) localised heating

Figure 2: Simulation scenarios to determine the range of power deposition necessary for annealing the tension spring, both upper and lower bounds.

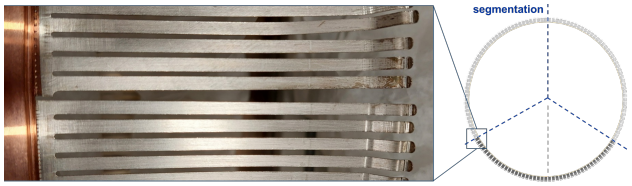

Figure 3: A sample photograph depicting the increased gap between two welded RF finger sheets.

lation approaches were explored via finite element method steady-state thermal simulations in COMSOL [7], as illustrated in Fig. 2: (a) a uniform power deposition across the entire spring and (b) a localised lumped power deposition over a cross-section of the spring, giving insights into the upper and lower bounds of the tension spring heating dynamics. The simulation analyses determined that achieving annealing conditions necessitates a power deposition of 27 W in the uniform case and 130 mW in the lumped case.

The power dissipated to heat the spring must originate from the circulating beam. However, the spring is positioned in the outer volume between the RF insert and the bellows; thus, it is shielded electromagnetically by the RF fingers. Nevertheless, it has commonly been assumed that in case of non-conformities in modules containing RF fingers, the EM shielding mechanism is altered [8]. Figure 3 depicts a photograph displaying a larger spacing of about 3 mm (twice the nominal gap size) between consecutive RF fingers. The reason is that the RF fingers were originally intended for fabrication from a singular copper beryllium sheet, bent into a circle of the intended diameter, and welded onto a copper holder. Mechanical constraints led to the segmentation of the single sheet into three distinct sections, causing irregularities upon welding at intervals of 120 ° in all ID212 WMs, with two larger spacings and one reduced spacing. Such asymmetry in the RF finger distribution impacts the EM field configuration, as elaborated in the subsequent section.

IMPEDANCE ASSESSMENT

One of the first steps of the impedance assessment involved bench measurements via the standard coaxial stretched wire method [9, 10] of the ID212 WM, as sketched in Fig. 4. A more detailed description of the setup is given

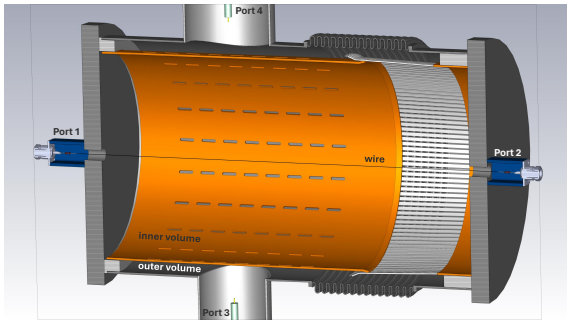

Figure 4: Schematic cross section of the wire method setup.

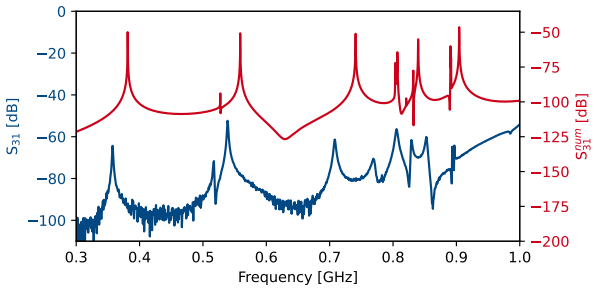

Figure 5: Comparison between measured (blue) and simulated (red) transmission coefficient $S_{31(32)}$- similar behaviour was observed for $S_{41(42)}$-.

in [11–13]. While this method is suitable for detecting resonant modes, quantifying the beam coupling impedance is not possible with bench measurement techniques due to setup limitations [12, 13]. Therefore, we strongly rely on EM simulations and the validation of the simulation model with the measurements is required. This is achieved by directly comparing the simulation model and the experimental measurements conducted by replicating the bench measurement setup in CST [14]. One of the first outcomes of the impedance assessment was detecting the EM-field leakage from the inner to the outer volume through the transition tube pumping slots and the RF finger gaps. This is demonstrated by the presence of low-frequency resonances below the beam pipe cut-off frequency (at about 1.1 GHz) detected through the measured transmission scattering parameter S_{31} (Port 1 to Port 3 at the vacuum access port of the module), as shown in Fig. 5 (solid blue line). Also, stemming from the frequency-domain simulations, the numerical transmission scattering parameter S_{31}^{num} (red solid line) confirms these resonances. Therefore, the virtual and real bench measurements exhibit a satisfactory agreement, especially considering the complexity of replicating the setup, including aspects such as the design of the RF fingers and the positioning of probes. The field leakage observed is identified as the possible mechanism for dissipating some of the beam-induced power on the spring. The determined low-frequency trapped resonant modes in the outer volume are associated with the length of the module. For instance, the first resonance at about 375 MHz is the so-called half-λ resonance based on

ISBN: 978-3-95450-247-9 ISSN: 2673-5490 doi: 10.18429/JACoW-IPAC2024-TUAN3

Figure 6: Beam-induced power range on the tension spring for three different scenarios using `bihc` [15].

the length of the module of about 400 mm. Axial stretching and compressing tests conducted (at the bench and virtually) exhibited the expected frequency shifts. In addition, all of these trapped modes fall within the relevant beam spectrum of the LHC [1], enhancing the power dissipation.

Once the numerical model was validated, a quantitative analysis of the beam impedance and resulting beam-induced power dissipated on the spring was followed. This analysis was completed considering various potential operational scenarios of the ID212 WM. Since two beams circulate through the module, horizontal beam offsets of up to 8 cm occur, depending on the installation location in the machine. As mentioned in the previous section, an asymmetry in RF finger distribution arises from mechanical constraints during fabrication, resulting in wider gaps between two consecutive RF fingers. The orientation of these additional gaps relative to the traversing beam position is random in the machine. Besides, a possible degradation of the contact between fingers and the transition tube is included, ranging from the 'ideal contact' to the extreme case of complete loss of contact. An intermediate contact quality, the 'degraded contact' case, is also considered. It describes the RF fingers starting to lose contact points with the transition tube, indicating that the electric contact is imperfect. This situation escalates to the 'lost contact' case, where one or more fingers have no contact and can potentially reach the extreme case where all fingers are disconnected.

Finally, the beam-induced power calculations are performed using the open-source python package `bihc` [15] and the beam parameters of the exact fill that caused the failure (Fill 8828). Since the modules are common beam chambers, the power loss is computed considering the two-beam case [16]. Figure 6 summarises the outcome of the investigation for the power dissipated on the tension spring ranging from the lowest values of 0.07 mW for the ideal contact case up to the extreme case of 200 W in the lost contact case. The framed region (dark blue dashed lines) could represent a plausible power range associated with the failed module condition. This range overlaps with the range indicated by the violet arrows, which represents the annealing condition for both localised and distributed power on the spring, respectively. Furthermore, EM simulations indicate the possibility of localised heating, as depicted in Fig. 7, particularly in the presence of wider gaps in the RF fingers distributions and beam offset. Since this situation aligns with the experienced issue, it could reasonably initiate the cascade of failures of the ID212 WM.

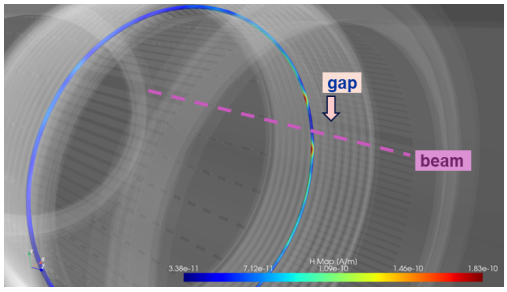

Figure 7: Localised H-field distribution on the spring around the defects region obtained from CST field monitors weighted by `bihc` beam-induced power computations [15].

MITIGATION STRATEGY

A systematic upgrade of the current 71 RF finger modules ID212.7 mm, employing newly designed counterparts wherever feasible, is being considered [17]. The current LHC configuration involves the placement of an ID212 WM every 5.5 m in the specific warm sectors to counteract axial movement during bake-out cycles. However, analyses indicate that reducing the number of modules could still effectively compensate for the total axial movement. Thus, the mitigation strategy entails a modular exchange based on positional requirements [11]. This involves utilising flexible modules, such as the deformable RF contact bridges (DRF) [18–20], and unshielded bellows [21], in areas of dynamic necessity [17]. Additionally, it involves employing robust fixed-length modules in possible static positions. In these modules the existing RF fingers are removed and replaced with a new solid taper-like copper transition. The new transition ring ensures electrical contact over an embedded spring [17]. It is thermally robust due to the material thickness (10 mm), and the impedance is expected to be similar to a straight vacuum chamber. The entire module is secured at a fixed length to allocate the thermal expansion during bake-out cycles to the designated flexible modules.

CONCLUSION

The investigation into the ID212 WM breakdown during the 2023 LHC run identified a cascade of failures, notably a cycle of localised tension spring heating and degradation in RF finger contact quality, ultimately leading to the loss of their electrical contact on the transition tube perimeter. Field leakage played a pivotal role in dissipating beam-induced power on the tension spring, particularly near enhanced RF finger spacing. The presence of a beam offset and the high beam intensity aggravate these effects. A mitigation strategy is being put in place to avoid future issues and LHC performance limitations in the High Luminosity era.

ACKNOWLEDGEMENTS

The authors would like to extend their sincere gratitude to the Impedance Working Group (IWG) members and EN-MME colleagues at CERN for their invaluable support and insightful discussions throughout this study.

ISBN: 978-3-95450-247-9 ISSN: 2673-5490 doi: 10.18429/JACoW-IPAC2024-TUAN3

REFERENCES

[1] E. Métral, "Beam-induced heating / bunch length / RF and lessons for 2012", in *Chamonix 2012 Workshop on LHC Performance*, pp. 105–115. doi:10.5170/CERN-2012-006.105

[2] B. Salvant *et al.*, "Beam induced RF heating", in *4th Evian Workshop on LHC beam operation*, 2012, pp. 109–118.

[3] E. Métral *et al.*, "Lessons learned and mitigation measures for the CERN LHC equipment with RF Fingers", in *4th International Particle Accelerator Conference (IPAC'13)*, Shanghai, China, May 2013, pp. 1802–1804. https://jacow.org/IPAC2013/papers/TUPWA042.pdf

[4] B. Salvant *et al.*, "Beam induced RF heating in LHC in 2015", in *Proc. 7th International Particle Accelerator Conference (IPAC'16)*, pp. 602–605. doi:10.18429/JACoW-IPAC2016-MOPOR008

[5] O. Santos, "Impact of Bake-out on RF module spring mechanical properties", CERN - EDMS No. 2959115, Tech. Rep., 2023.

[6] A. Galloro, G. Bregliozzi, and M. Morrone, "Thermal analysis of the VMBGA warm vacuum module", CERN - EDMS No. 2957992, Tech. Rep., 2023.

[7] COMSOLAB, *Comsol multiphyics 6.1*, https://www.comsol.de.

[8] O. Kononenko, B. Salvant, E. Métral, A. Grudiev, and F. Caspers, "Impedance studies for VMTSA module of LHC equipped with RF Fingers", in *Proc. 4th International Particle Accelerator Conference(IPAC'13)*, pp. 1805–1809.

[9] F. Caspers, "Impedance determination from bench measurements", CERN, Geneva, Switzerland, Rep. CERN-PS-2000-004-RF, Tech. Rep., 2000.

[10] V. G. Vaccaro, "Coupling impedance measurements: an improved wire method", INFN, Tech. Rep., 1994. https://cds.cern.ch/record/276443

[11] C. Antuono and P. Krkotić, "Limitations from LHC RF fingers ", presented at Joint Accelerator Performance Workshop 2023. https://indico.cern.ch/event/1337597/timetable/?view=standard

[12] C. Antuono *et al.*, "LHC RF fingers issue: status of the impedance studies", ABP Group Meeting, 2023. https://indico.cern.ch/event/1338806/

[13] C. Antuono *et al.*, "ABP note to be published under beam coupling impedance and beam induced heating of the LHC warm vacuum module", CERN, Tech. Rep., 2024.

[14] D. Systèmes, *CST Studio Suite 2023*. https://www.3ds.com/products/simulia/cst-studio-suite

[15] E. de la Fuente Garcia, F. Giordano, B. Salvant, L. Sito, and C. Zannini, *BIHC, A Python tool for beam induced heating computations*. https://github.com/ImpedanCEI/BIHC

[16] C. Zannini, G. Rumolo, and G. Iadarola, "Power loss calculation in separated and common beam chambers of the LHC", in *Proc. of 5th International Particle Accelerator Conference (IPAC'14)*, pp. 1711–1713. doi:10.18429/JACoW-IPAC2014-TUPRI061

[17] G. Bregliozzi, "Addressing known non-conformities LS3; RF (spring) bridges & warm bellows", Chamonix Workshop 2024. https://indico.cern.ch/event/1343931/contributions/5672971/

[18] C. Garion, A. Lacroix, and H. Rambeau, "Development of a new RF finger concept for vacuum beam line interconnections", in *Proc. 3rd International Particle Accelerator Conference (IPAC'12)*, pp. 2531–2533.

[19] J. P. Espinos and C. Garion, "Analysis and testing of a new RF bridge concept as an alternative to conventional sliding RF fingers in LHC", in *Proc. 7th International Particle Accelerator Conference (IPAC'16)*, pp. 3660–3662. doi:10.18429/JACoW-IPAC2016-THPMY006

[20] P. Krkotić *et al.*, "Impedance analysis of deformable RF contact bridges for high luminosity LHC", in *Proc. 14th International Particle Accelerator Conference (IPAC'23)*, pp. 3470–3473. doi:10.18429/JACoW-IPAC2023-WEPL153

[21] P. Krkotić and S. Calatroni, "Unshielded bellows warm modules", 83rd Impedance Working Group meeting. https://indico.cern.ch/event/1397685/